Kinematic and dinamic study of the suspension system of an electric single seater competition Formula Student

Estudio cinemático y dinámico del sistema de suspensión de un monoplaza de competencia eléctrico Formula Student

Christian Arévalo[1,*], Ayrton Medina[1], Juan Valladolid[1]

Abstract

The level of competitiveness generated by Formula Student has led to a series of studies and technological advances in order to improve the performance of single-seaters, so that their operation is successful according to the requirements of the competition. This document details the study of the suspension system of an electric Formula Student single-seater. This study involves an analysis of the kinematics and dynamics of the suspension system in which an analytical determination of movement, loads and vibrations is carried out by means of simulation software and mathematical calculations. The aim of the study is to evaluate the performance of the suspension according to the regulations of the competition, to establish parameters that improve the suspension system and at the same time the performance of the car in terms of comfort and safety.

Keywords: Single seater, Suspension, Dynamics, Kinematics.

Resumen

El nivel de competitividad que genera la Formula Student ha desencadenado en una serie de estudios y avances tecnológicos con el fin de mejorar cada vez más el rendimiento de los monoplazas para que se desenvuelvan con éxito ante las exigencias de la competencia. En este documento se detalla el estudio del sistema de suspensión de un monoplaza de competencia eléctrico Formula Student. Este estudio involucra un análisis de la cinemática y dinámica del sistema de suspensión en el cual se realiza una determinación analítica del movimiento, cargas y vibraciones por medio de software de simulación y de cálculos matemáticos. Con el estudio se busca evaluar el rendimiento de la suspensión en función del reglamento de la competencia, con el fin de establecer parámetros que mejoren el sistema de suspensión y a la vez el desempeño del monoplaza en términos de confort y seguridad.

Palabras clave: monoplaza, suspensión, dinámica, cinemática.

[1,*]Transport Engineering Research Group (GIIT), Automotive Mechanical Engineering Major, Universidad Politécnica Salesiana, Cuenca – Ecuador. Author for correspondence ✉: carevalom@est.ups.edu.ec.
 https://orcid.org/0000-0002-2906-3553, https://orcid.org/0000-0002-9172-7568,
 https://orcid.org/0000-0002-3506-2522.

1. Introduction

Formula Student is a student competition organized by the SAE (Society of Automotive Engineers) whose main objective is to promote the best training of young engineers [1], challenging university students to design, build and test the performance of a formula type vehicle that successfully meets the tests stipulated in the respective regulations [2], to then compete with other students around the world.

The technological advances and the level of competitiveness generated by Formula Student have motivated the UPS Racing Team of Universidad Politécnica Salesiana to develop two single-seater cars. The first one was a combustion car for the 2014 competition in the UK, while the second was an electric vehicle for the UK Formula Student Electric competition in 2017.

According to the results of last year [3], in the dynamic events the electric car has had problems with some mechanical and electrical systems; among the mechanical difficulties is the lack of adjustments in the settings and the suspension damping, as well as a failure located in a member of the lower control arm of the rear suspension.

Considering that the suspension plays a very important role in the performance of the vehicles in terms of safety and comfort, there is a need to carry out studies of the suspension that allow for improvements either in the development or in the design, so that the car can be competitive.

The main suspension design in competition is the deformable parallelogram (doublé A-arm or double wishbone), which can have three forms of spring-damper assembly activation, which are: direct, by means of a push-rod, or pull rod [4]. These suspension systems are simple in design, easy to adjust, resistant, have good adaptability and can be light if they are made with composite materials, which is why they are widely used by Formula 1 and Formula Student cars [5].

The suspension must incorporate a good kinematic design to keep the tire as perpendicular as possible to the pavement, to maintain optimal cushioning and adequate elasticity rates to keep the tire on the ground at all times. In addition, the components must be resistant so that they do not fail under static and dynamic loads [6–9].

The objective of this work is to carry out the dynamic and kinematic study of the suspension system of the Formula Student electric vehicle, by means of kinematic simulation programs and mathematical calculations, to determine the performance of the suspension and to establish improvements or solutions to the problems that arise during the study.

2. Materials and methods

2.1. Study vehicle

The vehicle used to study the suspension is a Formula Student electric competition car, as shown in Figure 1.

Figure 1. Formula Student electric single-seater

The dimensions of the car are shown in Table **??**.

Table 1. Dimensions of the electric single-seater

Especification	Dimension
Front track width	1200 mm
Rear track width	1180 mm
Wheelbase	1600 mm
Weight with pilot	345 kgf
Front weight distribution	45%
Back weight distribution	55%
Height of center of gravity	300 mm

2.2. Suspension system characteristics

The characteristics of the suspension system are shown in Table 2.

Table 2. Suspension system characteristics

Specification	Detail
Type of suspension system (Front/rear)	Deformable parallelogram
Activation system spring - shock absorber (Front/rear)	Push-rod
Stabilizer bar (Front/rear)	Sprat type
Shock absorbers (Front/rear)	Ohlins TTX25
Rigidity of the spring (front/front) (N/mm)	150/200
Total length of the boat/bounce suspension (mm)	30/30
Material	Carbon fiber and aluminum 7075 T6
Tires	19.5 x 7.5-10 (Hoosier), R25
Rims	7 in x 10 in (Braid), offset: +35

Arévalo et al. / Kinematic and dinamic study of the suspension system of an electric single seater competition Formula Student

97

2.3. eometric parameters

The coordinates of the connection points of each element of the suspension are as shown in Table 3. The connection points, in addition to allowing the definition of geometric parameters of the suspension, are necessary for the kinematics simulation program and for the 3D calculation of the forces in the members of the suspension.

Table 3. Coordinates of the connection points of the suspension's elements

Pts.	Front suspension			Rear suspension		
	X(mm)	Y(mm)	Z(mm)	X(mm)	Y(mm)	Z(mm)
P1	1443,9	212	227,59	15	250	203,59
P2	1732	212	227,59	335	250	203,59
P3	1730	520	218,83	148,83	555	219
P5	1446,6	256	377,59	15	290	347,59
P4	1732	256	377,59	335	290	347,59
P5	1760	520	400,83	171,17	529	401
P6	1710	480,74	244,78	148,83	513	241,8
P8	1710	295,72	509,03	148,83	308	628,68
P9	1790	520	218,83	220	549,14	259,83
P10	1750	190	227,59	220	258,5	234,2
P11	1710	61,21	534,99	148,83	70,51	660,02
P12	1710	238,98	534,99	148,83	245,98	660,2
P13	1760	520	310	160	541,98	310
P14	1760	590	310	160	600	310
P15	1699	238,38	468,88	159,83	245,98	596,42
P16	1721	238,38	468,88	137,83	245,98	596,42

Figure 2 shows the location of the connection points of the suspension elements.
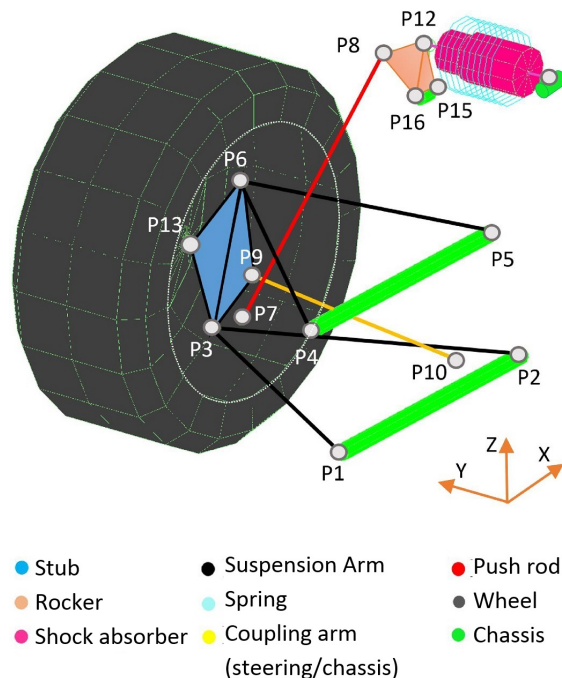

Figure 2. Location of the connection points of the suspension elements.

Table 4 shows the geometric parameters based on wheel dimensions, track gauge, wheelbase and the coordinates of the suspension connection points according to [6, 7].

Table 4. Geometric parameters of the suspension system

Parameter	Front suspension	Rear suspension
Height of the balancing center (mm)	44,84	70,02
Angle of advance (°)	7	9
Output angle (°)	8,13	0
Angle of fall (°)	0	0
Mechanical Trail (mm)	28,32	70,02
Scrub radius (mm)	24,56	0
Anti-sinking / (%) Anti-lifting	0	0

An analysis is made of the results of the FSAE TIRE TEST CONSORTIUM [10], referring to the Hoosier® tire 19.5 x 7.5-10, which is used in the study car. The analysis is carried out in order to determine the range of acceptable angles of fall, the behavior of the tire and a prediction of the maximum forces it can withstand. Figure 3 shows that the maximum lateral force is presented for an angle of fall of –1° to –1.3°, while the maximum longitudinal force is made for a fall of 0°. The tire does not suffer a sharp drop in grip after reaching the maximum peak, so an effective fall range of 1 to -3° can be set.
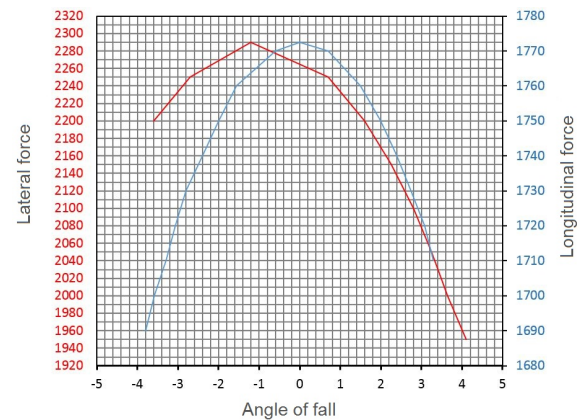

Figure 3. Angle of fall at different lateral and longitudinal forces, for a normal weight of 1000 N.

3. Results and kinematic analysis

Using Lotus Suspension Analisys, a kinematic analysis of the suspension system is performed. The program allows the user to know the behavior of the suspension with the geometry established on various stages in the track, such as bounce and rebound, roll and direction turn [11]. The parameters that are analyzed are those that characterize the behavior of the suspension [12], such as:

- Balancing center

- Angle of fall

- Angle of advance

- Toe (convergence/divergence)

For the simulation, the dimensions of the car and the coordinates of the connection points of each element of the suspension are inserted into the program. Lotus creates a three-dimensional model of the type of suspension to be analyzed as shown in Figure 4.
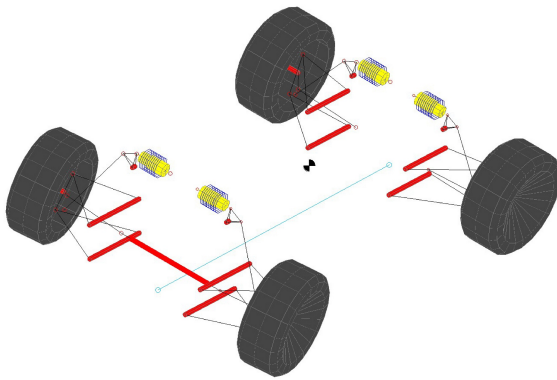

Figure 4. Simulated suspension system in Lotus Suspension Analysis.

The elevation or bounce of the suspension in the vertical direction is analyzed, which tries to simulate the passage of the car over a bump or obstacle of 30 mm in height. For this analysis, only the right wheel of the front and rear axle is considered, because the left wheels display a similar behavior.

Figure 5 shows that the front wheels in a bouncing situation have a maximum negative fall gain of -1.13°, and in rebound a maximum positive fall of 0.9°. The rear wheels in the bouncing situation have a maximum negative fall gain of -1.63°, and in rebound a maximum positive fall of 1.41°. The behavior of the angle of fall is favorable according to [13], because when the vehicle passes through a curve, the most loaded wheel will have a negative fall gain and the discharged wheel a positive fall gain, improving the lateral grip and its traction simultaneously. In order to achieve maximum performance of the tire and reduce the positive angle of fall, a static angle of fall for the front and rear wheels of -1° and -1.5° respectively can be established. Having a static fall, wheels with maximum compression approach a negative fall of -2.6°, staying within an effective range of 1° and -3°, according to the analysis of the tires. According to the recommendation of Carroll Smith [9], the static fall adjustment can be reduced by improving the grip of the tire in both curved and straight trajectories.
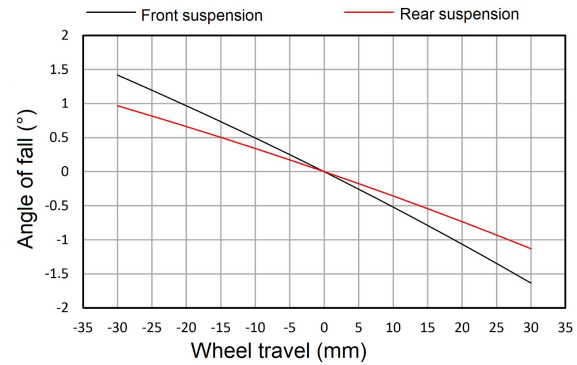

Figure 5. Variations of the angle of fall with wheel bounce and rebound.

According to Figure 6, the forward advancing angle becomes positive with the wheel bounce and negative with the rebound, while the rear advancing angle has a positive orientation in both bounce and rebound. The angle of advance contributes to the gain of the angle of fall during a turn. According to the results, during curves the angle of advance will cause the external wheel to have a negative fall gain and the fall of the internal wheel to trend to be positive.
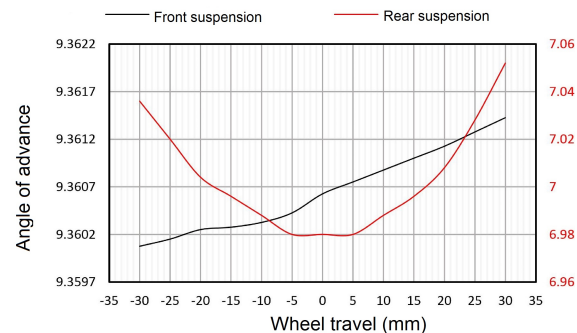

Figure 6. Variations of the angle of advance with wheel bounce and rebound.

Figure 7 shows that the maximum vertical travel of the center of balance with the bounce and rebound is 80.344 mm and 86.4 mm for the front and rear suspension respectively. The center of balance is maintained at all times above the ground plane, something very desirable according to [14]. The height of the center of balance to the center of gravity and the anti-roll effect of the elastic elements allow the angle of roll of the chassis to be 1° at a lateral acceleration of 1 G, without considering the deformation of the tires.
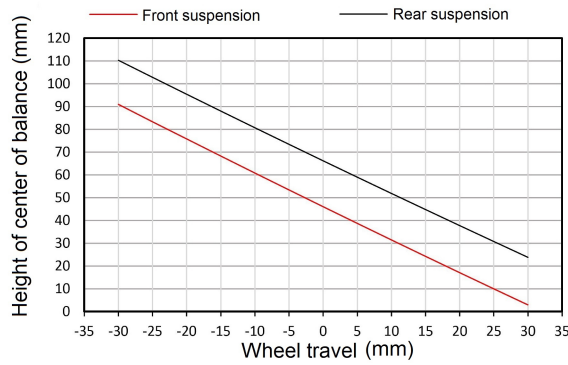
Arévalo et al. / Kinematic and dinamic study of the suspension system of an electric single seater competition Formula Student

99

Figure 7. Variations of the height of the center of balance with bounce and rebound of the wheel.

Figure 9. Variations of the angle of fall with rolling of the chassis.

The maximum rear toe is 0.1393 degrees with wheel rebound and maximum forward toe is 0.0328 degrees with wheel bounce, as shown in Figure 8. A slightly positive toe reduces rolling resistance and a negative toe improves maneuverability in curves, however, excessive toe increases tire wear. The low values are due to the fact that the bump steer effect is null, which has been achieved with a correct geometry of the steering rods.
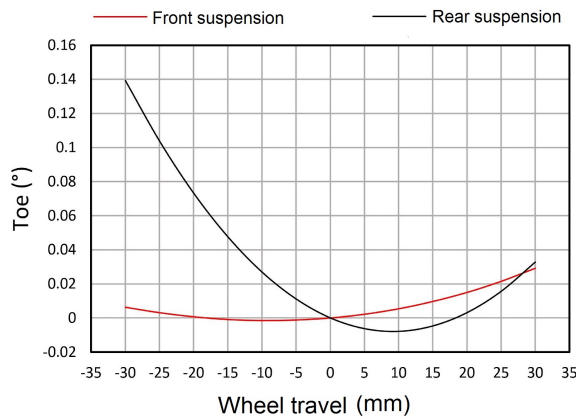
Figure 10 shows that the rear and front swing centers have a lateral travel of 186.44 mm and 119.05 mm respectively, with a maximum rolling of the chassis of 3°. Considering the effect in the reduction of the rolling of the elastic elements (springs and stabilizer bar), as well as a lateral acceleration of 1 G; the chassis will have 1° of roll, where the lateral migration of the balancing center will be 63.57 mm/G and 40.25 mm/G in the front and rear suspension respectively.

Figure 8. Toe variations with bounce and rebound of the wheel.

Figure 10. Lateral movement of the center of rolling with rolling of the chassis.

The passage of the car through a curve is simulated, which causes the suspension to tilt due to centrifugal acceleration. The lateral force is translated into a roll angle of the chassis. According to Figure 9, when the rolling of the chassis is positive the wheel is external to the curve and if it is negative the wheel is internal to the curve. With a rolling of 3° of the chassis, the maximum angle of fall for the external and internal wheel of the front axle is 1.28 and -1.52 degrees respectively, while in the rear axle the maximum angle of fall is 1,83° for the outer wheel and -2,01 for the inner wheel. Depending on the results, the wheels outside the curve have a negative fall gain, allowing for an improvement in tire grip.
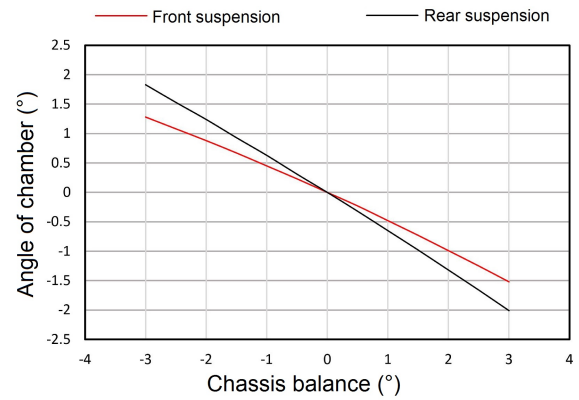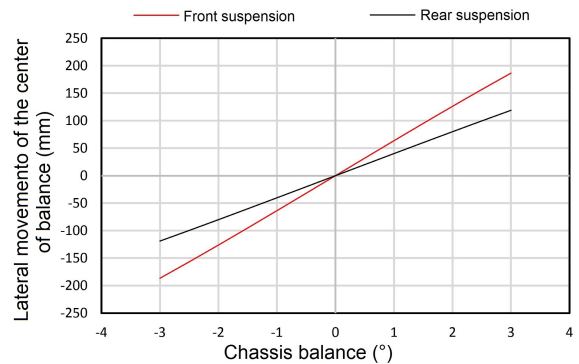
Figure 11 shows the behavior of the right front wheel with the turn of the direction. When the wheel is internal to the curve and with the maximum angle of rotation has a negative fall of -2.75°. If the wheel is external to the curve, a positive fall of 5.33° is generated with the maximum turn.

4. Results and dynamic analysis

The calculations of the forces generated in the members of the suspension system are performed when the vehicle is subjected to different dynamic load scenarios. It is important to consider as many scenarios as possible because the forces generated will vary for each member depending on the load case. Five different load scenarios are established to which the vehicle is subjected in a typical road environment [15].
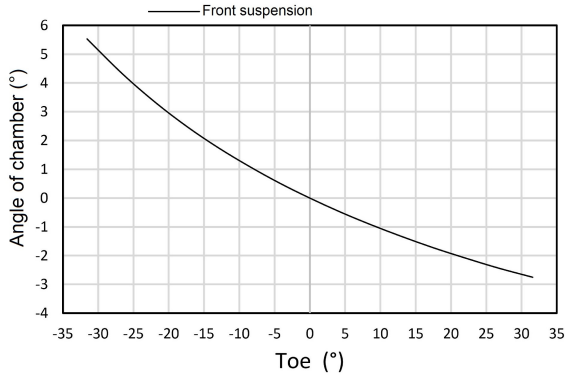
Figure 11. Variations of the angle of fall with the turn of the direction.

- Linear acceleration

- Linear braking

- Passing through curve

- Acceleration in curve

- Curved braking

- Passing through obstacle

For each load scenario, the forces generated in the referential system are calculated, X in longitudinal direction to the vehicle, Z in perpendicular direction to the ground and Y in the direction transverse to the vehicle. The forces that are generated in the tire patch in the X and Z directions due to acceleration and braking as shown in Figure 12, are defined by equations 1-6:
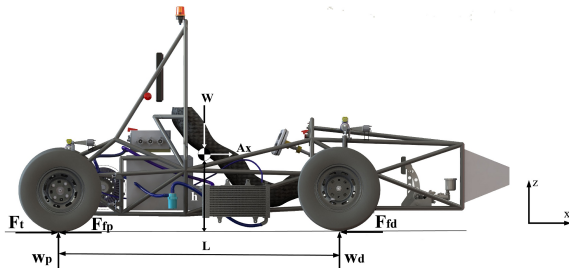

Figure 12. Forces present in the tire patch during acceleration and braking.

$$Ax = \frac{v_f - v_o}{t} \quad (1)$$

$$Ft = \frac{\frac{\mu \times W \times b}{L}}{1 - \frac{h}{L} \times \mu} \quad (2)$$

$$Ffp = \mu \times \left(W_e - \frac{W \times Ax \times h}{l} \right) \quad (3)$$

$$Ffd = \mu \times \left(W_e - \frac{W \times Ax \times h}{l} \right) \quad (4)$$

$$Wd = W_{ed} + \frac{W \times Ax \times h}{l} \quad (5)$$

$$Wp = W_{ep} - \frac{W \times Ax \times h}{l} \quad (6)$$

Where:
Ax = longitudinal acceleration (m/s^2)
v_o = initial speed (m/s)
v_f = final speed (m/s)
Ft = tensile force (N)
W = weight of the vehicle (N)
l = wheelbase (m)
h = height of the center of gravity (m)
μ = coefficient of adhesion
Wed = static weight on the front axle (N)
Wep = static weight on the rear axle (N)
Wd = dynamic weight on the front axle (N)
Wp = dynamic weight on the rear axle (N)
Ffd = braking force on the front axle (N)
Ffp = braking force on the rear axle (N)
b = distance from the axle posterior to the center of gravity (m)

The forces that are generated in the tire patch in the Y and Z directions due to the curve path as shown in Figure 13, are determined by equations 7, 8, 9.
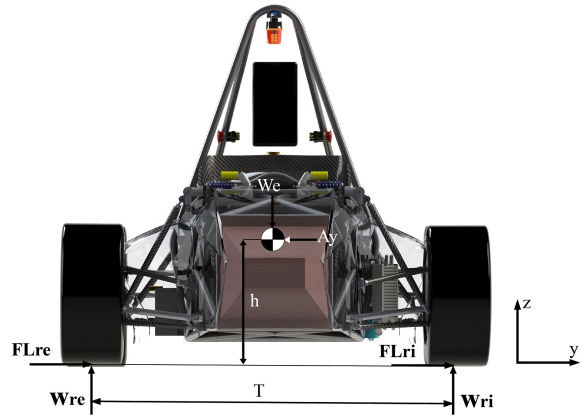

Figure 13. Forces present in the tire patch on the curve.

$$Fl = \frac{m \times v^2}{4 \times r} \quad (7)$$

$$w_{re} = \frac{W_e}{2} + \frac{W_e \times Ay \times h}{T} \quad (8)$$

$$Wp = W_{ep} - \frac{W \times Ax \times h}{l} \quad (9)$$

Where:
m = mass of the vehicle (kg)
v = vehicle speed (m/s)
r = radius of curvature (m)
Ay = lateral acceleration (m)
W_e = static weight on the axle (N)

W_{re}= dynamic weight on the outer wheel (N)

W_{ri}= dynamic weight on the inner wheel (N)

T = track width (m)

h = height of the center of gravity (m)

The forces generated in the tire patch in the Z direction due to passing through an obstacle are determined by equation 10:

$$F_{eje} = 0,2m_{axis} \times a_z \qquad (10)$$

Where:

F_{axis} = force on the shaft (N)

a_z =vertical acceleration (m/s^2)

m_{axis} = mass of the axis (kg)

With the established load scenarios, we proceed to determine the forces that are generated in the suspension members. In the front and rear suspension there are a total of six members, where two members are the upper control arm (BCS), two members of the lower control arm (BCI), one of the push-rod (PR) and one of the coupling arm (BA). For this analysis it is assumed that the load acts on the center of the wheel. The wheel center is considered to be the base of the rigid body and point (0,0,0) as shown in Figures 14 and 15.
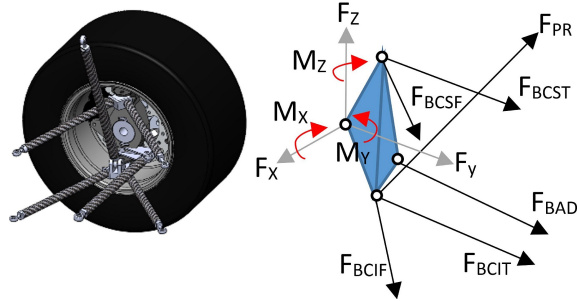

Figure 14. Free body diagram of the forces in the members of the front suspension.
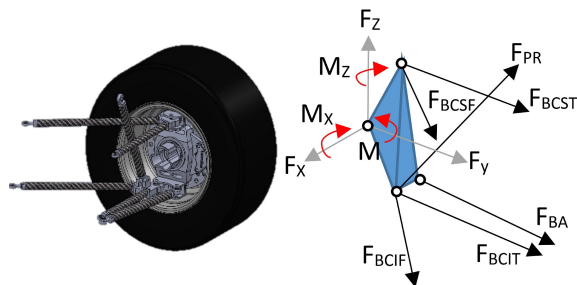

Figure 15. Free body diagram of the forces in the members of the rear suspension.

A system of vectors and matrices is used to determine how these forces are distributed along each of the suspension elements [16].

With a balance of forces and moments with respect to the X, Y and Z coordinate axes of the wheel center, six equations are determined. The system of equations is solved by the following expression:

$$[A]x = B$$
$$x = [A]^{-1}B \qquad (11)$$

x represents the unknown force in each of the suspension members.

$$x = \begin{pmatrix} F_{PR} \\ F_{BCSF} \\ F_{BCST} \\ F_{BCIF} \\ F_{UCST} \\ F_{BA/BAD} \end{pmatrix} \qquad (12)$$

B represents the forces and moments in X, Y and Z generated in the center of the tire patch and resolved on the center of the wheel.

$$B = \begin{pmatrix} F_x \\ F_y \\ F_z \\ Mx \\ My \\ Mz \end{pmatrix} \qquad (13)$$

The matrix A is determined by the unit vectors obtained from the sum of forces and momentsin the X, Y and Z directions of each member. The force vector $(\overrightarrow{F})$ is equal to the product point between the unit vector (u) and the magnitude of the force $(|F|)$, as shown in equation 15. The moment $(\overrightarrow{M})$ is equal to the cross product between the force vector $(\overrightarrow{F})$ and the moment arm vector $(\overrightarrow{r})$, as can be seen in equation 15.

$$\overrightarrow{F} = |F| \times \overrightarrow{u}$$
$$\overrightarrow{M} = \overrightarrow{F} \times \overrightarrow{r} \qquad (14)$$

$$\overrightarrow{M} = |F| \times \overrightarrow{u} \times \overrightarrow{r} \qquad (15)$$

$$[A] = \begin{bmatrix} u_{PRx} & u_{BCSFx} & u_{BCSTx} & \cdots \\ u_{PRy} & u_{BCSFy} & u_{BCSTy} & \cdots \\ u_{PRz} & u_{BCSFz} & u_{BCSTz} & \cdots \\ (u_zr_y - u_yr_z)_{PR} & (u_zr_y - u_yr_z)_{BCSF} & (u_zr_y - u_yr_z)_{BCST} & \cdots \\ (u_zr_x - u_xr_z)_{PR} & (u_zr_x - u_xr_z)_{BCSF} & (u_zr_x - u_xr_z)_{BCST} & \cdots \\ (u_yr_x - u_xr_y)_{PR} & (u_yr_x - u_xr_y)_{BCSF} & (u_yr_x - u_xr_y)_{BCST} & \cdots \end{bmatrix}$$

$$\begin{bmatrix} \cdots & u_{BCIFx} & u_{BCITx} & u_{BAx} \\ \cdots & u_{BCIFy} & u_{BCITy} & u_{BAy} \\ \cdots & u_{BCIFz} & u_{BCITz} & u_{BAz} \\ \cdots & (u_zr_y - u_yr_z)_{BCIF} & (u_zr_y - u_yr_z)_{BCIT} & (u_zr_y - u_yr_z)_{BA} \\ \cdots & (u_zr_x - u_xr_z)_{BCIF} & (u_zr_x - u_xr_z)_{BCIT} & (u_zr_x - u_xr_z)_{BA} \\ \cdots & (u_yr_x - u_xr_y)_{BCIF} & (u_yr_x - u_xr_y)_{BCIT} & (u_yr_x - u_xr_y)_{BA} \end{bmatrix} \quad (16)$$

Tables 5 and 6 show the maximum forces of tension and compression in the members of the suspension system, as a result of the different load scenarios. The maximum tensile forces in the members of the suspension arms are –4313 N and –5131 N in the front and rear respectively, and the maximum compression forces are 4165 N and 5119 N. The front and rear push-rods work only in compression where the forces are 5358 N and 8544 N for the front and rear respectively.

Table 5. Results of the forces on the members of the front suspension

Load scenarios	Forces on the members of the front suspension					
	FPR	FBCSF	FBCST	FBCIF	FBCIT	FBAD
Acceleration (N)	487	109	82	–272	–178	–58
Braking (N)	1149	4162	–2726	–2021	3350	–2623
Curve (N)	1092	–1160	–1459	1063	957	825
Acceleration and curve (N)	296	–1339	–1594	1508	1248	918
Braking and curve (N)	2495	1013	4165	146	–4313	–1109
Step through obstacle (N)	5358	1203	906	–2990	–1954	–629
Maximum force (N)	5358	4162	4165	–2290	–4313	–2623

Table 6. Results of the forces in the members of the rear suspension

Load scenarios	Forces in the members of the rear suspension					
	FPR	FBCSF	FBCST	FBCIF	FBCIT	FBAD
Acceleration (N)	1494	–3942	2874	4775	–5131	–776
Brakimg (N)	754	2582	–1333	–2437	988	482
Curve (N)	2239	998	–2225	–155	1297	-625
Acceleration and curve (N)	2090	–3168	238	5119	–2503	52
Braking and curve (N)	956	–1772	-949	3553	–153	–268
Step through obstacle (N)	8544	1646	1986	–2593	–2915	521
Maximum force (N)	8544	–3942	2874	5119	–5131	776

Compression and tensile tests are performed to determine if the limbs support the maximum calculated loads. In the tensile test, the bond strength between the aluminum grafts and the carbon fiber tube is measured [17]. The graft is an aluminum element glued with a high resistance adhesive to the carbon fiber tube, allowing the anchoring to the chassis or to the spindle by means of ball joints. The tubes are of two external diameters, 18.1 mm and 21.3 mm with a thickness of 1.15 mm. The larger diameter tube is used for the push-rod and the coupling arms. The smaller diameter tube is used for the suspension arms.

Table 7. Results of the compression and tensile tests of the members of the suspension

Tube diameter (mm)	Traction force (KN)	Fuerza Compression force (KN)
18,1	2,9	13,59
21,3	8,93	13,88

According to the results of Table 7, it can be said that the members of the suspension arms could fail in tension, since according to the tensile test, the maximum joint force is 2.9 KN, and the maximum tension force in one member of the suspension arm is –5.13 KN. In the case of compression, the members are subject to buckling, therefore, it is necessary to perform a calculation of critical buckling (P_{cr}) and safety factor (F_s), defined by equations 18 and 19. The calculation will make it possible to more accurately predict a case of compression failure [18].

$$P_{cr} = \frac{C\pi^2 El}{l^2} \quad (17)$$

$$F_s = \frac{P_{cr}}{c} \quad (18)$$

Where:
C = condition constant of articulated ends
P = axial force (N/m^2)
E= modulus of material elasticity (N/m^2)
I= moment of inertia (m^4)
l = length of the bar (m)
According to the results of Table 8, the members of the suspension arms, push-rod and coupling arm would

Arévalo et al. / Kinematic and dinamic study of the suspension system of an electric single seater competition Formula Student

103

not fail due to buckling effects since, according to the calculation, they have safety factors greater than 2 and support higher compression forces than 13 KN.

Table 8. Results of the calculation of critical buckling and safety factor of suspension members working by compression

Tube diameter (mm)	Buckling critical (N)	Axial force (N)	Security factor
18,1	14 181,35	5119	2,77
21,3	18 769,27	8544	2,19

Since one of the most important tasks of the suspension system is to absorb the irregularities of the road without losing traction in the tires, the vast majority of cars are equipped with shock absorbers and springs to fulfill this purpose. In this section, through a model of 2 degrees of freedom of the suspension system of ¼ of the vehicle [19], the analysis of the frequencies of the suspension is made, generating an interaction between the road and the vehicle. Figure 16 shows the model of the suspension of a quarter of the vehicle with 2

degrees of freedom, which includes the elastic constant of the tire, as well as the non-suspended mass. The position of the suspended mass is X_1, the non-suspended mass is X_2 and X_0 serves to model the unevenness of the terrain.
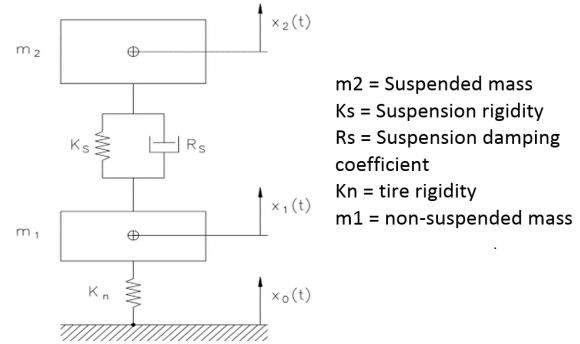

Figure 16. Full model of a quarter of a vehicle [11].

The transfer function of 2 degrees of freedom is given by the following expression:

$$\frac{x_2(s)}{x_0(s)} = \frac{R_s \cdot K_n \cdot s \cdot K_s \cdot K_n}{(m_1 \cdot s^2 + R_s \cdot s + K_s + K_n)(m_2 \cdot s^2 + R_s \cdot s + K_s) - (R_s \cdot s - K_s)^2} \tag{19}$$

With the defined modeling, the necessary initial parameters are established to allow the study to be carried out, as shown in Table 9.

Table 9. Parameters of the model of a quarter of a vehicle

Parameter	Front suspension	Rear suspension
m2: suspended mass (kg)	61,1	74,75
Ks: suspension rigidity (N/m)	26 220,47	34 960,62
Rs: suspension damping coefficient (Ns/m)	....	....
Kn: tire stiffness (N/m)	102 917,699	132 322,756
m1: mass not suspended (kg)	10,9	13,25
MR: motion ratio	1,3	1,4
Kw: wheel stiffness (N/m)	15515,071	17837,051
fm2: natural frequency of the suspended mass (Hz).	2,36	2,3
fm1: natural frequency of the unsuspended mass (Hz)	16,62	16,81
Ccr: critical damping coefficient (Ns/m)	2487,28	3233,274

The force developed by a shock absorber (F_a) is represented by the equation:

$$F_d = R_s \cdot v_p \tag{20}$$

Where:

R_s = damping coefficient [Ns/m]

v_p = speed on the piston of the shock absorber [m/s]

Using mathematical Matlab software, the transmissibility of the suspension system is analyzed at

different damping coefficients for high and low speed provided by the TTX 25 damper [20]. By means of equation 23 and the graph in Figure 17, the slopes or damping coefficients for the different damper settings are determined as shown in Table 10.
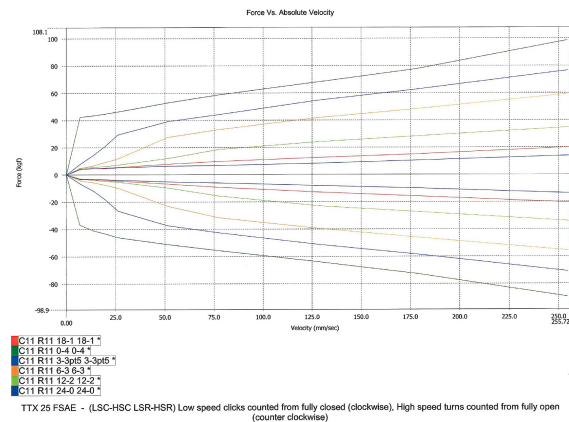

Figure 17. Damping coefficients for different shock absorber settings [21]

To maximize the traction area, the lowest possible transmissibility is required. The graphics of Figures 18 and 19 show the response of the second-degree model of the front and rear suspension. It can be seen that if the damping factor is increased at low input frequencies, the transmissibility is reduced to the maximum, which means that the tire will not lose traction. After the point of intersection, the low damping factors result

in a lower transmissibility, attenuating movement in the chassis [22].

Table 10. Damping coefficients for different shock absorber settings

Adjustment of the shock absorber	Low speeds slope [KN*s/m]	High speeds slope [N*s/m]
C11 R11 0-4	52,788	2223
C11 R11 3-3pt5	11,77	1962
C11 R11 6-3	5,282	1831
C11 R11 12-2	2,354	882,9
C11 R11 18-1	3,678	689,1
C11 R11 24-0	3,678	567,5

According to the transmissibility analysis, a high damping factor is necessary (ξ) at low speeds and a low value for high speeds in the shock absorber. The TTX25 shock absorber, for the front suspension, needs a very close value of $\xi = 0,73$, which is achieved with setting C11 R11 6-3 for low speed. For high speeds the setting C11 R11 24.0 provides un $\xi = 0,22$. In the rear suspension a value of $\xi = 0,68$ is required, which is achieved with the C11 R11 0-4 setting for low speed. For high speeds the setting C11 R11 18.1 provides un $\xi = 0,22$.
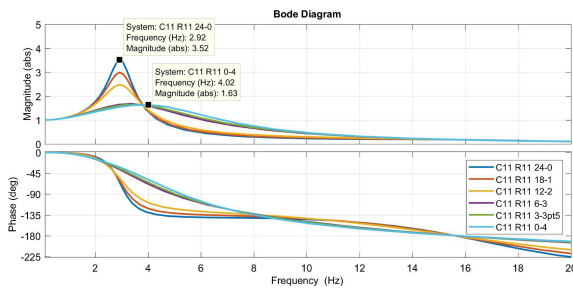

Figure 18. Transmissibility of the second-degree model of the front suspension.

As the system moves both compression and extension, according to [23] it is better to have a damping factor lower than compression and greater than extension in relation to the desired value in order to avoid resonance in the system (see Figure 20).
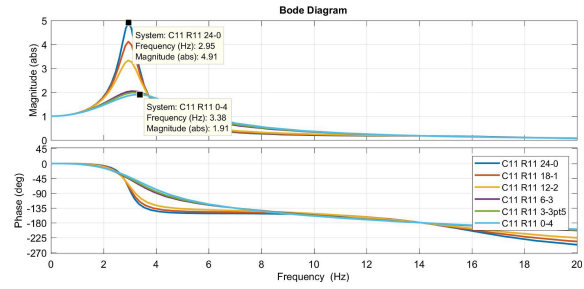

Figure 19. Transmissibility of the second-degree model of the rear suspension.
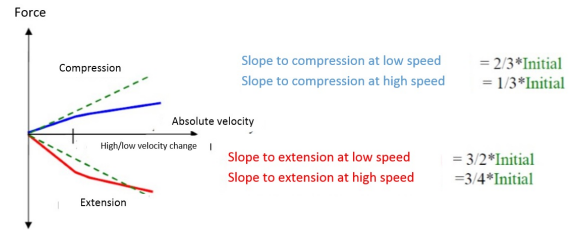

Figure 20. Slope adjustment for high speeds and low speeds. [23]

According to the analysis made, the use of double the compression damping factor for extension is determined. In this way, it is possible to achieve a good grip of the wheel, a lower transmissibility and better maneuverability. The calibrations that meet these requirements are shown in Tables 11 and 12.

Table 11. Damping factor of the front suspension

Adjustment of shock absorberr	Compression		Extension	
	Low speed	High speed	Low speed	High speed
C11 R11 12-2	0,92	0,34	......	......
C11 R11 6-3	......	......	2,08	0,72

Table 12. Factor de amortiguamiento de la suspensión posterior

Adjustment of shock absorberr	Compression		Extension	
	Low speed	High speed	Low speed	High speed
C11 R11 12-2	0,72	0,27	......	......
C11 R11 6-3	......	......	1,63	0,56

Figures 21 and 22 show the system response of the front and rear suspension respectively in front of a vertical displacement as input. It can be seen that the calibrations of the low speed damping factor in compression attenuate oscillations in the shortest time possible with respect to other calibrations.
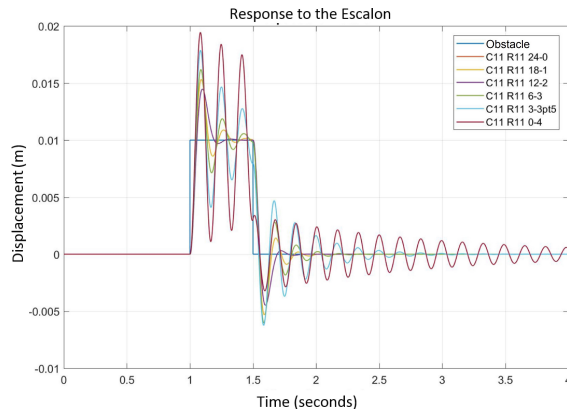
Arévalo et al. / Kinematic and dinamic study of the suspension system of an electric single seater competition Formula Student

105

Figure 21. Response of the front suspension system to a vertical displacement as input.
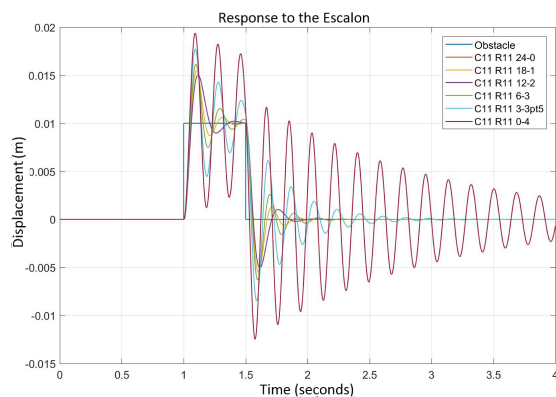

Figure 22. Response of the rear suspension system to a vertical displacement as input.

5. Conclusions

This research helps to have a broader view of the suspension systems used by FSAE competition vehicles. With the study of the kinematics, the behavior of the suspension of the car was determined under different scenarios on the track, such as passing through a curve or an obstacle. Depending on the results, it can be said that the configuration provided for the single-seater's suspension allows a good directional control of the vehicle (null bump steer effect) and an adequate negative fall gain of the wheel with the travel of the suspension or rolling of the chassis, giving a good lateral grip to the tires. However, with the turn of the steering there is a gain of excessive positive fall in the front wheels, which would affect the lateral grip in very tight corners. With the appropriate adjustments in the angles of advance, exit, static fall and convergence, the required or optimal conditions of vehicle stability and steering could be ensured, allowing greater accelerations, better braking and faster cornering steps. According to the study of the forces in the members of the suspension with dynamic loads, it was determined

that the suspension arms subjected to stress loads can fail in critical cases, the problem is in the strength of the joints between the aluminum grafts. With the second-degree model of a quarter of a vehicle and with the help of Matlab, a transmissibility analysis was carried out that allowed defining the characteristics that the shock absorber must have to guarantee maximum contact area, which produces greater traction.

References

[1] IMechE. Formula student. Institution of Mechanical Engineers. [Online]. Available: https://goo.gl/Mkjf9n

[2] S. International. (2017) Formula sae rules. [Online]. Available: https://goo.gl/pSeNqe

[3] Formula Studente Germany. (2017) Formula student electric - world ranking list. Mazur Events+Media. [Online]. Available: https://goo.gl/2Q75AE

[4] A. Staniforth, *Competition Car Suspension: Design, Construction, Tuning*, Haynes, Ed., 1999. [Online]. Available: https://goo.gl/2jhg7s

[5] Rapid-Racer. (2016) Suspension. [Online]. Available: https://goo.gl/5Dpwjr

[6] W. F. Milliken and D. L. ;illiken, *Race Car Vehicle Dynamics*, S. International, Ed., 1995. [Online]. Available: https://goo.gl/iuhFqJ

[7] T. Pashley, *How to Build Motorcycle-engined Racing Cars*, V. P. Ltd, Ed., 2008. [Online]. Available: https://goo.gl/XdxRGM

[8] M. Royce and S. Royec, *Learn & Compete: A Primer for Formula SAE, Formula Student and Forumula Hybrid Teams*, R. Graphic, Ed., 2012. [Online]. Available: https://goo.gl/9rxtrG

[9] C. Smith, *Tune to Win*, C. S. Consulting, Ed., 1978. [Online]. Available: https://goo.gl/KaTkxq

[10] Milliken Research. (2018) Formula sae tire test consortium. Milliken Research Associates Incorporated. [Online]. Available: https://goo.gl/ErGrP5

[11] G. P. Pillajo Quijia, "Estudio cinemático del comportamiento de la suspensión de un prototipo de formula sae student eléctrico del equipo upm racing," Master's thesis, Universidad Politécnica de Madrid. España, 2012. [Online]. Available: https://goo.gl/aTb5mt

[12] P. De la fuente aguilera, "Análisis de la suspensión del vehículo monoplaza eléctrico UPM-03e del equipo UPM racing," Universidad Politécnica de Madrid. España., 2016. [Online]. Available: https://goo.gl/PvvCV3

[13] S. Juvanteny Gimenez, "Estudio y diseño del sistema de suspensión para un prototipo de fórmula sae," Tesis de grado. Universidad Politécnica de Cataluña. España, 2015. [Online]. Available: https://goo.gl/q93zhh

[14] E. I. Efler herranz, "Diseño de la suspensión trasera de un vehículo formula student," Tesis de grado. Universidad Politécnica de Madrid. España, 2016. [Online]. Available: https://goo.gl/YkgNnv

[15] E. D. Flickinger, "Design and analysis of formula sae car suspension members," Master's thesis, California State University, Northridge. EEUU, 2014. [Online]. Available: https://goo.gl/tcUw5g

[16] L. Borg, "An approach to using finite element models to predict suspension member loads in a formula sae vehicle," Master's thesis, Virginia Polytechnic Institute and State University. USA, 2009. [Online]. Available: https://goo.gl/i8bV4B

[17] A. C. Cobi, "Design of a carbon fiber suspension system for fsae applications," Bachelor thesis. Massachusetts Institute of Technology. USA, 2012. [Online]. Available: https://goo.gl/h1tQU3

[18] R. G. Budynas and J. K. Nisbett, *Diseño en ingeniería mecánica de Shigley*, 9th ed., M. Mc Graw-HILL, Ed., 2012. [Online]. Available: https://goo.gl/dumukn

[19] F. Aparicio Izquierdo, *Teoría de los vehíulos automóviles*, E. T. S. d. I. I. Universidad Politécnica de Madrid, Ed., 1995. [Online]. Available: https://goo.gl/M2EHoy

[20] J. Hurel, E. Teran, F. Flores, and B. Flores, "Modelo físico y matemático del sistema de suspensión de un cuarto de vehículo," in *15th LACCEI International Multi-Conference for Engineering, Education, and Technology. USA*, 2017. [Online]. Available: https://goo.gl/7yrFEK

[21] ́OHLINS. (2017) Ttx25 mkii,. ́OHLINS. Advanced Suspension Technology. [Online]. Available: https://goo.gl/Kra2dB

[22] A. Espejel Arroyo, "Rediseño de un sistema de suspensión para un auto de competencia mediante adams/car y matlab," Tesis de grado. Universidad Nacional Autónoma de México, 2015. [Online]. Available: https://goo.gl/sTxBg9

[23] M. Giariffa and S. Brisson, "Tech tip: Spring & dampers, episode four. a new understanding," OPTIMUMG. Vehicle dynamics solutions, Tech. Rep., 2017. [Online]. Available: https://goo.gl/kVkg6o